

# Slow light with flat or offset band edges in multi-mode fiber with two gratings

Andrey A. Sukhorukov<sup>1</sup>, C. J. Handmer<sup>2</sup>, C. Martijn de Sterke<sup>2</sup> and M. J. Steel<sup>3,2</sup>

ARC Center of Excellence for Ultrahigh-bandwidth Devices for Optical Systems (CUDOS),

<sup>1</sup> Nonlinear Physics Centre, Research School of Physical Sciences and Engineering, Australian National University, Canberra, ACT 0200, Australia

<sup>2</sup> School of Physics, University of Sydney, Camperdown, NSW 2006, Australia

<sup>3</sup> RSoft Design Group, Inc., 65 O'Connor St, Chippendale, NSW 2008, Australia

[ans124@rsphysse.anu.edu.au](mailto:ans124@rsphysse.anu.edu.au)

**Abstract:** We consider mode coupling in multimode optical fibers using either two Bragg gratings or a Bragg grating and a long-period grating. We show that the magnitude of the band edge curvature can be controlled leading to a flat, quartic band-edge or to two band edges at distinct, nonequivalent  $k$ -values, allowing precise control of slow light propagation.

© 2018 Optical Society of America

**OCIS codes:** (050.2770) Gratings; (060.2310) Fiber optics

---

## References and links

1. J. T. Mok, C. M. de Sterke, I. C. M. Littler, and B. J. Eggleton, "Dispersionless slow light using gap solitons," *Nature Physics* **2**, 775–780 (2006).
2. X. Letartre, C. Seassal, C. Grillet, P. Rojo Romeo, P. Viktorovitch, M. L. d'Yerville, D. Cassagne, and C. Jouanin, "Group velocity and propagation losses measurement in a singleline photonic-crystal waveguide on InP membranes," *Appl. Phys. Lett.* **79**, 2312–2314 (2001).
3. A. Figotin and I. Vitebskiy, "Gigantic transmission band-edge resonance in periodic stacks of anisotropic layers," *Phys. Rev. E* **72**, 036619–12 (2005).
4. M. Ibanescu, S. G. Johnson, D. Roundy, C. Luo, Y. Fink, and J. D. Joannopoulos, "Anomalous dispersion relations by symmetry breaking in axially uniform waveguides," *Phys. Rev. Lett.* **92**, 063903–4 (2004).
5. M. Ibanescu, S. G. Johnson, D. Roundy, Y. Fink, and J. D. Joannopoulos, "Microcavity confinement based on an anomalous zero group-velocity waveguide mode," *Opt. Lett.* **30**, 552–554 (2005).
6. Y. Cao, R. Hudgins, T. J. Suleski, M. A. Fiddy, J. Raquet, K. Burbank, M. Graham, and P. Sanger, "1-D Photonic Crystal Exhibiting Degenerate Band Edge to Slow Light," In *Slow and Fast Light Technical Digest*, p. ME16 (Optical Society of America, Washington DC, 2006).
7. A. Yu. Petrov and M. Eich, "Zero dispersion at small group velocities in photonic crystal waveguides," *Appl. Phys. Lett.* **85**, 4866–4868 (2004).
8. D. Mori and T. Baba, "Wideband and low dispersion slow light by chirped photonic crystal coupled waveguide," *Opt. Express* **13**, 9398–9408 (2005), <http://www.opticsinfobase.org/abstract.cfm?URI=oe-13-23-9398>.
9. J. U. Kang, X. B. Xie, and J. Khurgin, "Group velocity modified Ti-diffused LiNbO<sub>3</sub> waveguides with dual Bragg gratings," *Electron. Lett.* **38**, 1049–1051 (2002).
10. T. Erdogan and J. E. Sipe, "Tilted fiber phase gratings," *J. Opt. Soc. Am. A* **13**, 296–313 (1996).
11. S. K. Case, "Coupled-wave theory for multiply exposed thick holographic gratings," *J. Opt. Soc. Am.* **65**, 724–729 (1975).
12. V. Mizrahi and J. E. Sipe, "Optical-properties of photosensitive fiber phase gratings," *J. Lightwave Technol.* **11**, 1513–1517 (1993).
13. A. Yariv, "Frustration of Bragg reflection by cooperative dual-mode interference: a new mode of optical propagation," *Opt. Lett.* **23**, 1835–1836 (1998).
14. K. S. Lee and T. Erdogan, "Fiber mode conversion with tilted gratings in an optical fiber," *J. Opt. Soc. Am. A* **18**, 1176–1185 (2001).

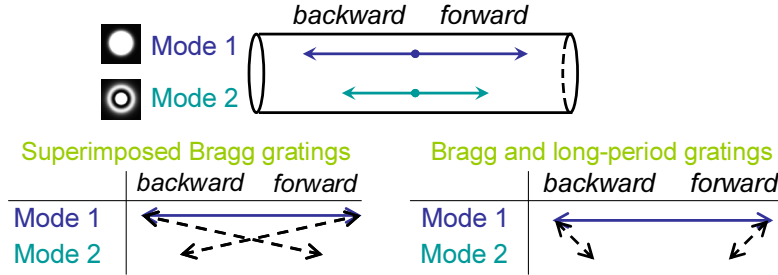


Fig. 1. Schematic of the coupling between the forward and backward propagating modes in a guided-wave structure using two superimposed Bragg gratings or Bragg and long-period gratings. Top: schematic of mode wavenumbers. Bottom: Solid and dashed arrows indicate mode coupling by individual gratings.

The ability to control the propagation of waves using the strong geometrical dispersion in photonic structures opens new opportunities for manipulating optical pulses. In particular, the regime of slow light can be achieved when the wavelength is tuned close to the edges of a photonic band-gap, as was demonstrated both in one-dimensional [1] and two-dimensional [2] geometries. The properties of slow-light modes strongly depend on the shape of the dispersion curve: if the curvature at the band edge is eliminated, to lowest order  $\omega - \omega_E \propto k^4$ , where  $\omega_E$  is the band-edge frequency and  $k$  the wavenumber. This results in a flat band-edge for which the group velocity  $v_g \propto k^3 \propto (\omega - \omega_E)^{3/4}$ . In addition, the curvature can be made to change sign so that the band edges appear at distinct non-equivalent  $k$ -values.

A flat band edge can lead to high energy densities and to an increased density of states at frequencies near the band edge [3, 4], with associated changes in the radiative properties of sources. The increase in the energy density is associated with fact that for a given, low group velocity pulse, the range of  $k$  values in a quartic band is larger than in a quadratic band, so that the pulse can be more strongly compressed in space. The increased density of states directly follows from the flattened shape of the dispersion relation. Slow modes with non-vanishing phase velocities can also be used to create high- $Q$  resonators [5]. It was earlier shown that such dispersion characteristics can be achieved in extended multi-layer anisotropic structures [3, 6] or omni-guide fibers [4, 5]. Flexible control of higher-order dispersion is also possible in photonic-crystal waveguides [7, 8].

In this work, we suggest a generic approach for the engineering of flat and offset band-edges in conventional fibers based on the grating coupling of forward- and backward-propagating modes of two different symmetries, *i.e.*, 4 modes in total. In the most common geometry in such structures, a Bragg grating is used to couple the fundamental mode to itself, leading to Bragg reflection and the opening of a (one-dimensional) photonic bandgap. The manipulation of this gap requires an additional degree of freedom, which is obtained by coupling two modes (such as the fundamental mode and a higher-order mode) using an additional grating, either a Bragg grating, or a long-period grating (see Fig. 1). This is somewhat similar to earlier proposals [3, 6], however in that work, a thin-film geometry in which the additional field has a different polarization was considered. Our proposal is based on effects which cannot be achieved with a dual Bragg grating [9] optimized only for a single guided mode. The suggested design does not require the use of anisotropic layers [3, 6] or a special fiber configuration [4, 5], being readily accessible with established grating-writing methods in conventional optical fibers.

We consider an optical fiber supporting two different modes,  $\mathcal{M}_1$  and  $\mathcal{M}_2$  (for example,

LP<sub>01</sub> and LP<sub>02</sub>). In the vicinity of a chosen frequency  $\tilde{\Omega}$ , their dispersion relations are given by  $\Omega_1 = \pm V_1(K_1 - \tilde{K}_1)$ ,  $\Omega_2 = \pm V_2(K_2 - \tilde{K}_2)$ . Here the  $\Omega_j$  are the frequency detunings from  $\tilde{\Omega}$ ,  $K_j$  are corresponding wavenumber shifts,  $V_j$  are the (positive) group velocities, and  $\tilde{K}_j (> 0)$  are reference wavenumbers at  $\tilde{\Omega}$ . The signs  $+$  and  $-$  correspond to forward and backward propagating waves, respectively.

As mentioned, we introduce a grating supporting the simultaneous resonant coupling of two pairs of forward- and backward-propagating modes  $\mathcal{M}_1$  and  $\mathcal{M}_2$ . This can be achieved with a superimposed modulation of the refractive index along the fiber

$$\Delta n(x, y, z) = \Delta n_1 \cos[\kappa_1 z + \phi_1] R(x, y) + \Delta n_2 \cos[\kappa_2 z + \phi_2] R(x, y), \quad (1)$$

where the  $R(x, y)$  defines the photosensitive cross-section of the fiber. We choose  $\kappa_1 = 2\tilde{K}_1 + \delta_1$  and  $\kappa_2 = \tilde{K}_1 + \sigma\tilde{K}_2 + \delta_2$ . Here  $\delta_j$  are small detunings from the two resonances, and  $\sigma = \pm 1$ . In both cases a Bragg grating with wavevector  $\kappa_1$  couples the forward- and backward-propagating  $\mathcal{M}_1$  mode. When  $\sigma = +1$  an additional Bragg grating couples the counter-propagating modes  $\mathcal{M}_1$  and  $\mathcal{M}_2$ , whereas for  $\sigma = -1$  the co-propagating modes are coupled by a long-period grating. The modulation amplitudes  $\Delta n_1$  and  $\Delta n_2$  define the coupling strengths between the  $\mathcal{M}_1$ - $\mathcal{M}_1$  and  $\mathcal{M}_1$ - $\mathcal{M}_2$  modes, respectively. Whereas it was previously found that multi-mode coupling and conversion with superimposed Bragg gratings can give rise to special features in the reflection and transmission spectra [10, 11, 12, 13, 14], we demonstrate below that the suggested superlattice modulation configuration enables new possibilities for dispersion control of band-edge slow-light states.

We assume that the structure is much longer than the beat length between the two modes,  $L \gg |\tilde{K}_2 \pm \tilde{K}_1|^{-1}$ ,  $|\tilde{K}_1|^{-1}$ ,  $|\tilde{K}_2|^{-1}$ , which is satisfied under typical conditions. Then, the pulse propagation can be modeled by the coupled-mode equations [10, 12] for the envelopes of the forward and backward propagating modes. Writing the electric field as

$$\mathbf{E}(x, y, z, t) = \{\mathbf{g}_1(x, y)[u_1(z, t) \exp(i\tilde{K}_1 z) + w_1(z, t) \exp(-i\tilde{K}_1 z)] + \mathbf{g}_2(x, y)[u_2(z, t) \exp(i\sigma\tilde{K}_2 z) + w_2(z, t) \exp(-i\sigma\tilde{K}_2 z)]\} \exp(-i\tilde{\Omega}t) + \text{c.c.}, \quad (2)$$

where  $\mathbf{g}_{1,2}(x, y)$  are transverse profiles for the two modes and c.c. denotes the complex conjugate, we see that the forward-propagating envelopes are  $u_1$  and  $u_2$  for  $\sigma = +1$  or  $w_1$  and  $w_2$  for  $\sigma = -1$ , and the backward-propagating envelopes are  $w_1$  and  $w_2$  for  $\sigma = +1$  or  $u_1$  and  $u_2$  for  $\sigma = -1$ . We choose the scaling where the normalized intensities define the energy density of modes per unit length of the fiber, and obtain the dimensionless equations

$$\begin{aligned} i \frac{\partial u_1}{\partial t} + iV_1 \frac{\partial u_1}{\partial z} + \rho_1 w_1 \exp(i\delta_1 z + i\phi_1) + \rho_2 w_2 \exp(i\delta_2 z + i\phi_2) &= 0, \\ i \frac{\partial w_1}{\partial t} - iV_1 \frac{\partial w_1}{\partial z} + \rho_1 u_1 \exp(-i\delta_1 z - i\phi_1) + \rho_2 u_2 \exp(-i\delta_2 z - i\phi_2) &= 0, \\ i \frac{\partial u_2}{\partial t} + i\sigma V_2 \frac{\partial u_2}{\partial z} + \rho_2 w_1 \exp(i\delta_2 z + i\phi_2) &= 0, \\ i \frac{\partial w_2}{\partial t} - i\sigma V_2 \frac{\partial w_2}{\partial z} + \rho_2 u_1 \exp(-i\delta_2 z - i\phi_2) &= 0. \end{aligned} \quad (3)$$

Here the (real-valued) grating strengths  $\rho_j$  are approximately given by

$$\rho_j = \frac{\pi \Delta n_j}{\lambda_0} \int \int_{-\infty}^{\infty} dx dy R(x, y) \mathbf{g}_1(x, y) \cdot \mathbf{g}_j(x, y), \quad (4)$$

with  $\lambda_0 = 2\pi c/\tilde{\Omega}$ . Note that the values of  $\rho_j$  can be chosen independently by selecting the strength of corresponding grating modulations and that Eqs. (3) satisfy the

energy-conservation condition,  $\partial(|u_1|^2 + |w_1|^2 + |u_2|^2 + |w_2|^2)/\partial t = \partial(-V_1|u_1|^2 + V_1|w_1|^2 - \sigma V_2|u_2|^2 + \sigma V_2|w_2|^2)/\partial z$ .

The dispersion relation of the system can be calculated by analyzing the eigenmodes of Eqs. (3) in the form,

$$\begin{aligned} u_1 &= U_1 \exp[i(k + \delta_1/2)z - i\omega t + i\phi_1/2], \\ w_1 &= W_1 \exp[i(k - \delta_1/2)z - i\omega t - i\phi_1/2], \\ u_2 &= U_2 \exp[i(k - \delta_1/2 + \delta_2)z - i\omega t - i\phi_1/2 + i\phi_2], \\ w_2 &= W_2 \exp[i(k + \delta_1/2 - \delta_2)z - i\omega t + i\phi_1/2 - i\phi_2]. \end{aligned} \quad (5)$$

We present the eigenmodes as sums of symmetric and antisymmetric vectors,  $U_j = F_{j+} + F_{j-}$  and  $W_j = F_{j+} - F_{j-}$  for  $j = 1, 2$ . After substituting these expressions into Eqs. (3), and obtaining the eigenmode equations, we find that they can be formulated in the matrix form

$$M_+ \begin{pmatrix} F_{1+} \\ F_{2+} \end{pmatrix} = k \begin{pmatrix} F_{1-} \\ F_{2-} \end{pmatrix}, \quad M_- \begin{pmatrix} F_{1-} \\ F_{2-} \end{pmatrix} = k \begin{pmatrix} F_{1+} \\ F_{2+} \end{pmatrix}, \quad (6)$$

where

$$M_{\pm} = \begin{pmatrix} (\omega \pm \rho_1)/V_1 - \delta_1/2, & \pm \rho_2/V_1 \\ \pm \rho_2\sigma/V_2, & \omega\sigma/V_2 + \delta_1/2 - \delta_2 \end{pmatrix}. \quad (7)$$

Therefore,  $k^2$  are eigenvalues of a square  $2 \times 2$  real-valued matrix  $M = M_+M_-$ . Thus there appear four branches of dispersion curves  $\omega_j(k)$ , with symmetry  $\omega_j(k) = \omega_j(-k)$ . For convenience, we label the branches such that  $\omega_1 \leq \omega_2 \leq \omega_3 \leq \omega_4$ . From the form of the matrices  $M_{\pm}$ , we observe that the dispersion does not depend on the grating phases  $\phi_j$ , and identify the symmetry property  $\omega_j(k; \delta_1, \delta_2, \rho_1, \rho_2, V_1, V_2) = \rho_1 \omega_j(kV_1/\rho_1; 0, \delta_2 V_1/\rho_1 - \delta_1 V_1[1 + \sigma V_1/V_2]/[2\rho_1], 1, \rho_2/\rho_1, 1, V_2/V_1) + \delta_1 V_1/2$ . Then, in the analysis and figures below we take  $\delta_1 = 0$ ,  $V_1 = 1$  and  $\rho_1 = 1$ , since for other values the dispersion curves can be obtained by simple scaling.

Away from the grating resonances,  $\omega_j(k \rightarrow \pm\infty) \simeq \pm V_{1,2}k$ , i.e., there are two pairs of branches with positive and negative frequency detunings. Since all  $\omega_j(k)$  are real for real  $k$ , branches cannot merge or disappear. However, for some frequencies all  $k$  can become imaginary, such that the propagation of linear waves is suppressed due to Bragg reflection. Such a photonic band-gap appears between the second and third branches and due to the symmetry of the dispersion curves, the band-gap edges appear at pairs of dispersion points labeled  $(\pm k_2, \omega_2^{(b)})$  (lower) and  $(\pm k_3, \omega_3^{(b)})$  (upper edge). The wavenumbers  $\pm k_2$  and  $\pm k_3$  define the corresponding phase velocity of slow-light modes.

To determine the features of band-edge dispersion, we first analyze the point with  $k = 0$ . Then, Eqs. (6) decouple, and admit solutions in the form of purely symmetric or antisymmetric modes when  $\text{Det}\{M_{\pm}[\omega_j(k=0)]\} = 0$ , the solutions of which satisfy

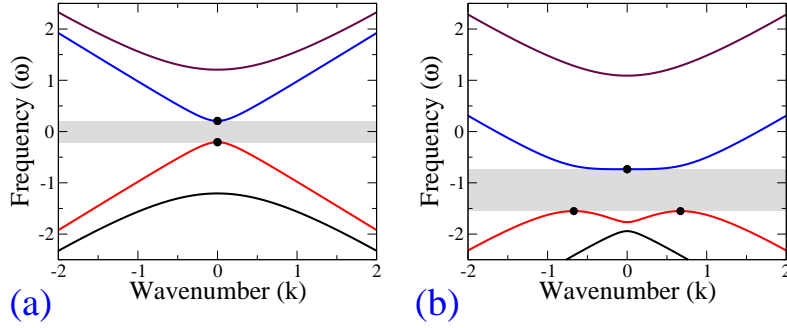
$$(\omega_j \pm 1)(\omega_j/V_2 - \sigma\delta_2) = \rho_2^2/V_2. \quad (8)$$

The dispersion points  $\omega_j(k=0)$  at  $j = 2$  or  $j = 3$  correspond to the edges of the photonic band-gap if the second eigenvalue of  $M[\omega_j(k=0)]$  is negative, i.e. if no other propagating modes exist in the spectral region around  $\omega_j(k=0)$ . This condition is satisfied if

$$\eta_j = (\omega_j/V_2 - \sigma\delta_2)^2 + (\omega_j^2 - 1) - 2\sigma\rho_2^2/V_2 < 0. \quad (9)$$

Therefore,  $\omega_j^{(b)} = \omega_j(k=0)$  and  $k_j = 0$  if  $\eta_j < 0$ . By choosing the grating strength and detuning, this can be realized at either of the band-edges [see examples in Figs. 2(a) and (c)], or at

## Superimposed Bragg gratings



## Bragg and long-period gratings

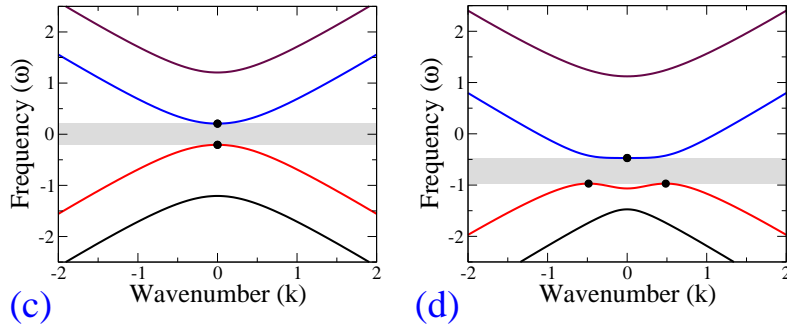


Fig. 2. Dispersion relation for structures based on (a), (b) two Bragg gratings ( $\sigma = +1$ ) and (c), (d) Bragg and long-period gratings ( $\sigma = -1$ ). Shading marks the band-gap, and filled circles indicate the band edges. For all the plots,  $V_1 = 1$ ,  $V_2 = 0.95$ ,  $\rho_1 = 1$ ,  $\rho_2 = 0.5$ ,  $\delta_1 = 0$ . Grating detunings are (a)  $\delta_2 = 0$ , (b)  $\delta_2 = -1.765$ , (c)  $\delta_2 = 0$ , (d)  $\delta_2 = 0.995$ .

a selected band-edge [upper band-edge in Figs. 2(b) and (d)]. In contrast, if  $\eta_j > 0$ , the sign of the curvature changes sign and the edges of the band-gap appear at points with non-zero wavenumbers  $\pm k_j$ , as at the lower gap edges in Figs. 2(b) and (d).

A key characteristic of slow-light at the band-edges is the second-order dispersion  $D = d^2\omega/dk^2$ . We find that the absolute value of  $D[\omega_j(k=0)]$  is proportional to  $|\eta_j|$ . Therefore, the dispersion at the gap-edge becomes quartic when  $\eta_j = 0$  as  $\omega_j = \omega_j(k=0) + 0 \times k^2 + O(k^4)$ , and this happens precisely at the transition of dispersion curves from the single band-edge with  $k_j = 0$  to double band-edges with  $\pm k_j \neq 0$ . The quartic dispersion occurs at the upper gap-edges in Figs. 2(b),(d).

In Fig. 3, we present the dependence of the wavenumbers ( $k_j$ ) and second-order dispersion at the band-gap edges. We note that Eqs. (6) and (7) possess a general symmetry,  $\omega(k; \delta_2) = -\omega(k; -\delta_2)$ , allowing us to represent simultaneously the characteristics for both the upper and lower band-edges. Results of calculations for superimposed Bragg gratings [Figs. 3(a),(b)] or Bragg and long-period gratings [Figs. 3(c),(d)] demonstrate that both the wave-number and dispersion of band-edge slow light can be engineered by choosing the grating detuning ( $\delta_2$ ) and strength ( $\rho_2$ ), the values of which can be freely selected by specifying the required grating period and the refractive index contrast. Consistent with the theoretical predictions, the absolute value of  $D$  is reduced to zero [visible as white stripes in Figs. 3(b) and (d)] along the path in the  $\delta_2 - \rho_2$  plane where band-edge wavenumbers  $k_j$  start to deviate from zero.

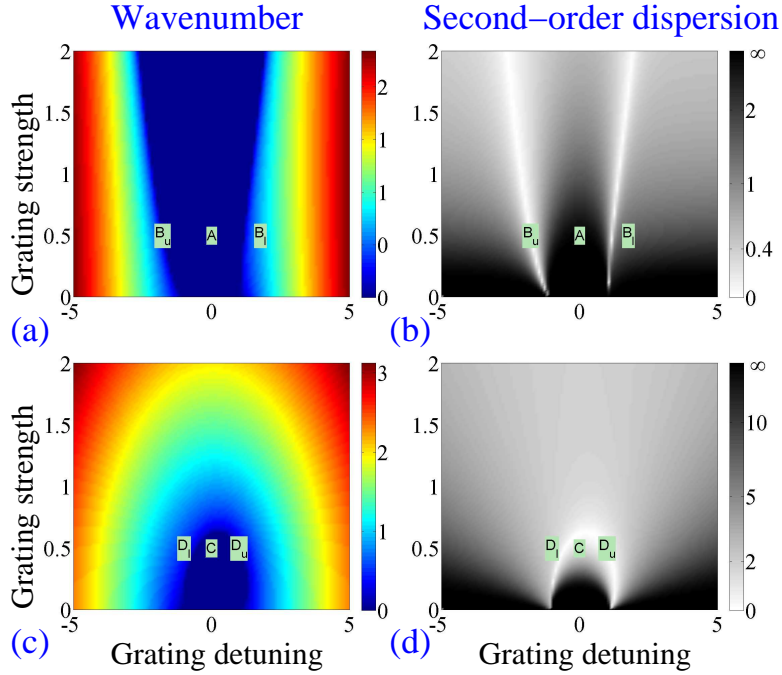


Fig. 3. Tuning characteristics of slow-light modes for (a),(b) coupled Bragg gratings ( $\sigma = 1$ ) and (c),(d) coupled Bragg and long-period gratings ( $\sigma = -1$ ). Shown are the dependencies of the absolute values of the band-edge (a,c) wavenumber and (b,d) group-velocity dispersion on the grating strength ( $\rho_2$ ) and detuning ( $+\delta_2$  at upper or  $-\delta_2$  at lower gap edges). Marked points A–D correspond to the dispersion plots in Figs. 2(a)–(d), respectively, where the subscripts  $u$  and  $l$  indicate the upper and lower gap edges (points A and C do not have subscripts as they coincide for both band-edges). Note that in (a) and (c), the band-edge wavenumbers are exactly zero throughout the dark blue region. Normalized parameters are the same as in Fig. 2.

We note that in Eq. (1) we assumed that the grating planes are orthogonal to the fiber axes. It was pointed out by Erdogan and Sipe [10] that by tilting these planes the coupling between selected modes can be enhanced. However, the detailed design of the grating is outside the scope of this work.

We stress that the technology for writing gratings in optical fibres is mature and the fabrication of the gratings described here should not be a problem, in principle. An additional degree of freedom that can be brought to bear in possible experiments is that the frequency difference between the resonances associated with the two gratings can be tuned by stretching the fiber.

In conclusion, we have demonstrated that both the phase velocity and the strength of second-order dispersion in the slow-light regime can be controlled in optical fibers with superstructured Bragg gratings or Bragg and long-period gratings designed for coupling of fundamental and higher-order modes. In particular, it is possible to realize flat band-edge dispersion of quartic type, when the second-order dispersion is suppressed. As a final point, though we considered here an optical fiber geometry, any multi-moded guided-wave geometry in which gratings can be fabricated is suitable for dispersion control of slow-light.

This work has been supported by the Australian Research Council through the Centre of Excellence CUDOS research projects.